Caving 2010 — Y. Potvin (ed)

doi:10.36487/ACG_rep/1002_34_Albrecht

# Application of advanced numerical modelling techniques for the assessment of caveability, subsidence and airblast hazard in a sublevel cave mine

**J.B. Albrecht** *AMC Consultants Pty Ltd, Australia*

**W.H. Gibson** *AMC Consultants Pty Ltd, Australia*

**A. Vakili** *AMC Consultants Pty Ltd, Australia*

**M.P. Sandy** *AMC Consultants Pty Ltd, Australia*

**K. Ross** *Red Back Mining Inc., Canada*

## Abstract

*As part of a feasibility study for a sublevel caving mine, a range of numerical modelling codes was used to study the major geotechnical risks involved. The key objectives of the numerical modelling study included: crown pillar stability assessment, hangingwall caveability assessment, surface subsidence analysis and investigation of the potential airblast hazard. Finite difference, finite element and distinct element methods were used for the modelling analysis in this study.*

*The numerical analyses indicated that continuous caving of the hangingwall was unlikely and that negligible surface subsidence would occur. An assessment of airblast hazard was also conducted as part of this study, using the results of the hangingwall stability analysis together with some theoretical calculations. The results of this study were used to design suitable airblast barricades and to quantify the minimum height of broken rock material required above each draw point location to reduce the airblast hazard to an acceptable level.*

*The results of the analyses described above were incorporated into a formal risk assessment to evaluate and rank the inherent risks in the project, including those associated with geomechanics aspects.*

## 1 Introduction

AMC Consultants (AMC) was commissioned by Chirano Gold Mines (Chirano) as part of the feasibility assessment of the Akwaaba underground mine to conduct a detailed numerical study to investigate the major geotechnical risks involved.

The Akwaaba deposit forms part of the Chirano Gold Mine operated by Chirano Gold Mines Limited in southwestern Ghana. The underground resource is located below the existing Akwaaba pit. The orebody dips generally at 70–75° to the west, is between 12–45 m thick and has an average strike length of 260 m. The current proposed mining extends to a depth of 500 m below surface.

Previous studies had identified longitudinal sublevel caving (SLC) as the preferred mining method for the Akwaaba underground orebody. SLC is an attractive method for this ore body as it provides early production, relatively simple design and drill-and-blast layouts, relatively few slots compared to the other stoping options, no backfill costs and no requirement for a footwall drive. These are all attractive features relative to the most obvious alternatives, i.e. sublevel open stoping or bench stoping.

Figure 1 illustrates the Akwaaba SLC underground mine and proposed access development, the existing open pit and the surface topography. The SLC will retreat in a continuous inclined front, mined from north to south, avoiding the formation of any closure pillars.

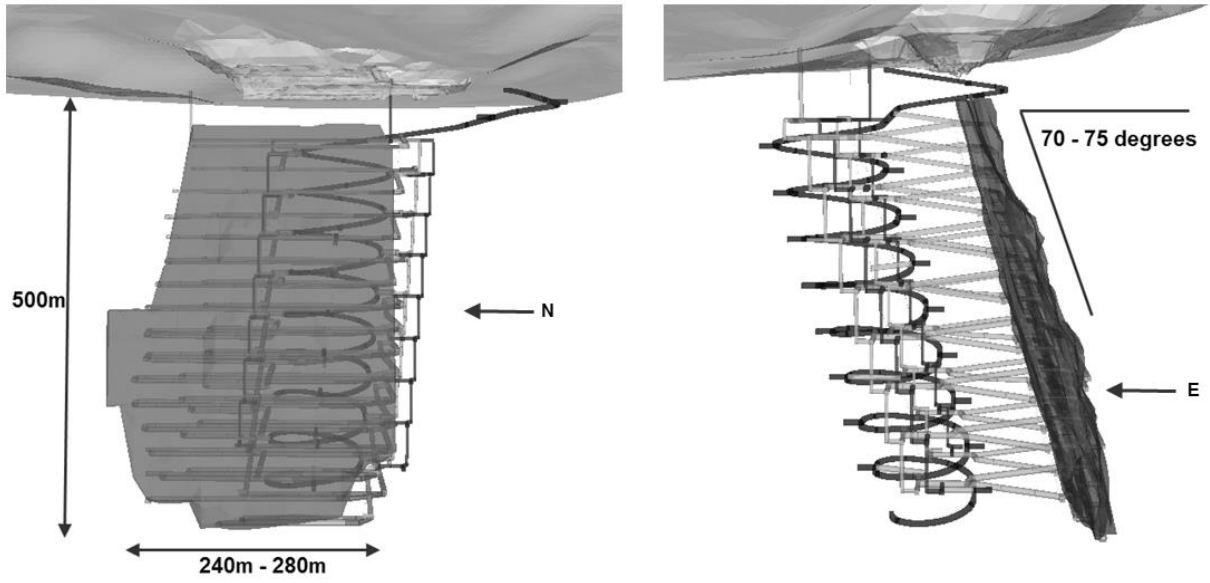


**Figure 1 Long-section and cross-section views of the Akwaaba underground mine**

The preliminary empirical assessment indicated that caving would be difficult in the good quality hangingwall (HW) rock mass. While traditionally this would exclude SLC as a viable method, SLC was selected on the proviso that a blanket of broken rock was to be maintained above the extraction level to prevent brows being drawn open and minimise the exposure of operators to rock fall and airblast hazards. Airblast barricades would also be required in all drives intersecting the SLC void positioned above the broken rock blanket. The method might be more appropriately described as 'pillarless uphole bench stoping, with deferred draw'. In this paper however, the term SLC is used.

The impact of leaving a permanent crown pillar below the open pit and the SLC, in a zone of low grade material (Figure 2) was also evaluated. The advantage of leaving the crown was to improve hangingwall stability, reduce the likelihood of surface subsidence, reduce uncontrolled water inflows into the underground mine, and reduce the potential for mud rushes.

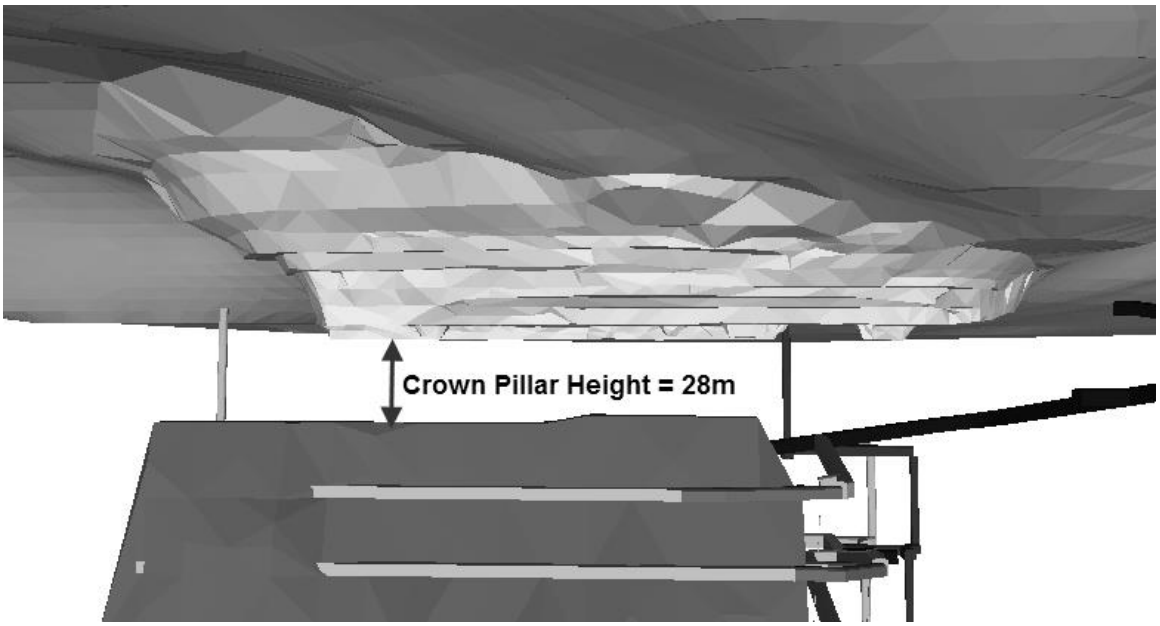


**Figure 2 Long-section of Akwaaba pit and underground showing the position and dimensions of the crown pillar (looking east)**

The main disadvantage of leaving the crown is the potential for sudden hangingwall collapse, airblast and mud rush if the crown pillar was to suddenly fail.

To better assess the likelihood of caving and other major geotechnical risks involved, various advanced numerical modelling simulations were conducted.

## 2 Modelling objectives

The main objectives of the modelling included:

- the assessment of crown pillar stability, caveability of the hangingwall and the extent of surface subsidence
- the assessment of the extent of yield in the abutments of the SLC for a range of face retreat angles
- the assessment of the airblast hazard.

## 3 Model descriptions

In this study both continuum and discontinuum analysis techniques were used. The continuum codes used included Dassault Systèmes finite element code Abaqus (Dassault Systèmes, 2009), and Itasca's finite difference code FLAC3D (Itasca, 2006). The distinct element code 3DEC (Itasca, 2007) was used for the discontinuum analysis. All of these models were mine scale, 3D and incorporated inelastic material models. The modelled geometries included accurate surface topology and final pit geometry based on survey information.

The continuum codes Abaqus and FLAC3D were used to assess crown pillar stability, caveability, surface subsidence and the extent of rock mass yield in the abutments of the SLC. The extent of abutment yield is used to determine suitable stand-off distances for capital infrastructure and dilution estimates for the SLC.

Figure 3 shows the finite element mesh and mine geometry modelled. In this study, three SLC face retreat angles (30, 40 and 60°) were considered, as well as a range of material properties based on the expected range of rock mass qualities derived from geotechnical logging data. Figure 4 shows the three face retreat angles modelled.

The distinct element code 3DEC was primarily used to identify the location, size and timing of potential unstable rock blocks that could form in the walls of the SLC. These potentially unstable blocks could present an airblast hazard if they were to detach and fall into the SLC void. The results of this study formed the basis of the airblast hazard assessment.

A 3DEC model (Figure 5) was developed based on the large scale continuous fault structures identified from pit and underground mapping at Akwaaba, and from interpretation of the drill hole logging information. To reduce the uncertainties in the material properties, a range of strength values (i.e. range of friction angles and dilation angles) were modelled. It was also assumed that all the modelled faults are fully persistent and planar.

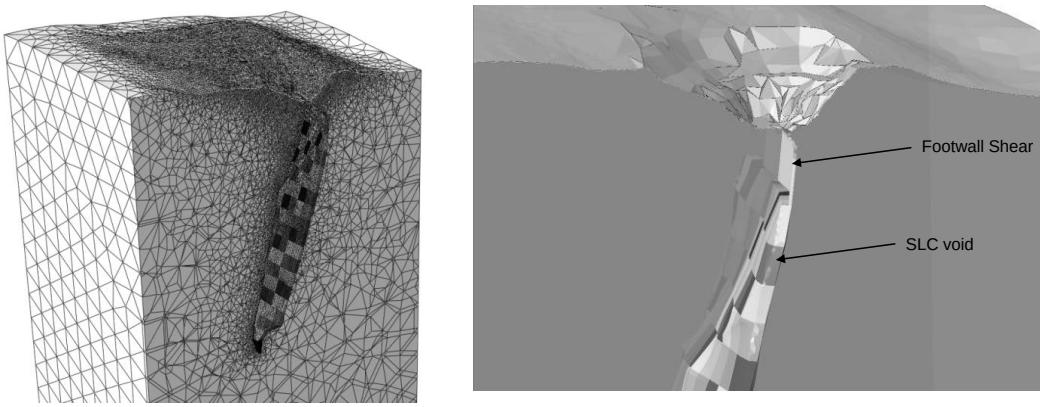


**Figure 3 The finite element mesh and mine geometry modelled**

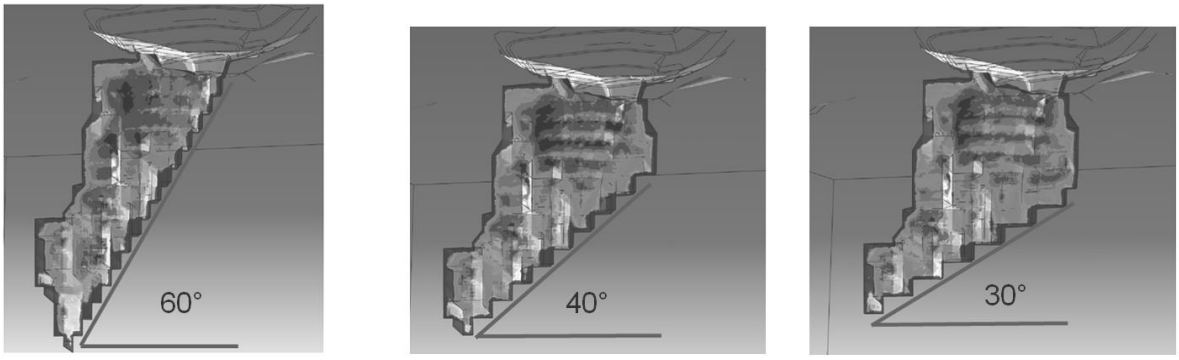


**Figure 4 Long-sections of the Akwaaba SLC showing the three SLC face retreat angles considered in the modelling**

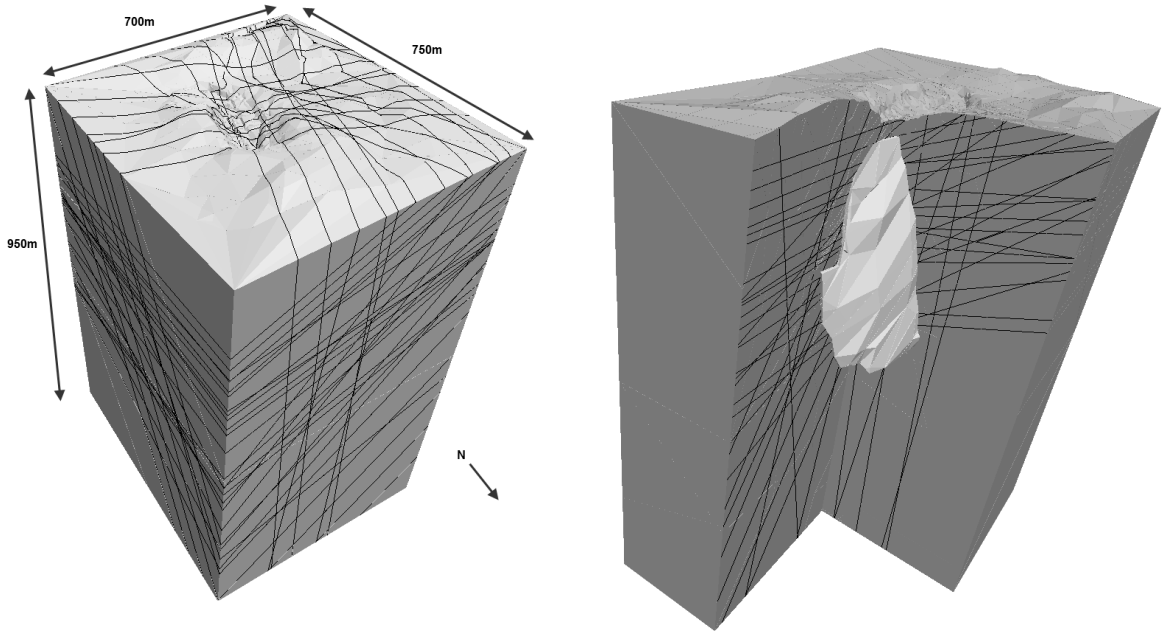


**Figure 5 3DEC model geometry showing the orientation of discontinuities modelled**

# 4 Geotechnical conditions

Formal assessment of the ground conditions in the orebody and host rocks was made using the Norwegian Geotechnical Institute's rock mass classification scheme (NGI Q). The rock mass classification assessment was based on a large database of geotechnical logging, based on 40 exploration drill holes, all of which were logged for Q parameters as well as structural orientations.

The orebody is comprised of strongly silicified brecciated volcanics and granitoids. Q values are generally 'very good'. A prominent shear lies in the immediate footwall of the mineralisation (Figure 3). The shear zone is more structured, with Q values in the range of 3.8–5.6, with ground conditions described as 'poor' to 'fair'. The shear is generally not rehealed and caving can be expected to break back to the more competent ground to the east of the shear. Some of the falloff is likely to be unmineralised.

The hangingwall (HW) domain is defined as the ground immediately adjacent to the hangingwall (within 50 m) of the main ore zone, and is comprised predominantly of volcanics and metasediments, with varying degrees of silicification and recrystallisation. Typical hangingwall conditions are associated with Q values of around 22–33 indicating good rock mass conditions.

The footwall (FW) domain is defined as the zone to the east of the footwall shear and comprises a sequence of quartz-rich arenites and minor conglomerates of Tarkwaian age. Visual inspection of the rock mass conditions in the existing decline development and exposure of the Tarkwaain sequence in the Akwaaba open pit, indicate that the ground conditions are generally 'good'.

For all domains considered, the jointing is widely spaced and most joints are planar and rough, with quartz, calcite or 'no' infilling. Several large-scale fault structures were identified from pit and underground mapping at Akwaaba. These structures are typically infilled with a narrow zone of weak infill material. The orientation of the dominant joint sets is shown in Figure 6.

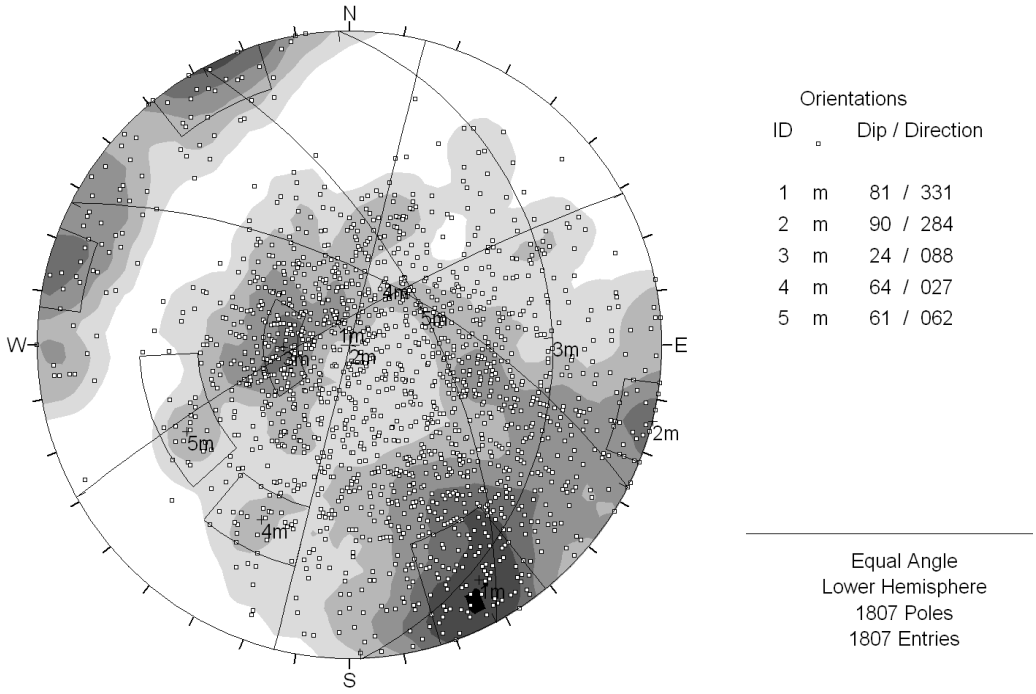


**Figure 6 Pole plot of major planes identified from analysis of mapping and logging data**

## 4.1 Material properties and rock mass strength

The procedure recommended by Hoek et al. (2002) was used to assess the rock mass strength based on material properties derived from rock mass classification and laboratory results. The rock mass strength was defined using a linear Mohr–Coulomb envelope based on the best fit, non-linear Hoek–Brown failure criteria at the expected levels of confinement.

As this is a new underground mine, there were no relevant observational or measurement data to calibrate the rock mass strength properties. As such a parametric approach was used, whereby a worst, expected and best case rock mass strength was quantified for each rock mass domain to account for the uncertainty in the modelled properties used in this study. The worst, expected and best case properties were based on the range of rock mass qualities derived from geotechnical logging data. Tables 1, 2 and 3 show the material properties and strength parameters for the expected case for each rock type included in the model.

For the Abaqus and FLAC3D models, the strength of the rock mass in close proximity to the open pit was degraded to account for the strength loss due to blast disturbance and the stress relief from overburden removal. The disturbance factor 'D' (Hoek et al., 2002) was used to degrade the rock mass in this situation. Fully disturbed properties were assumed for the immediate pit surface (i.e. D = 1.0), with the strength increasing linearly with depth, to the non-disturbed values at 15 m below the pit floor.

For the 3DEC models, the modelled discontinuities were defined used the large scale continuous fault structures identified from pit and underground mapping, and from interpretation of the drill hole logging information.

Due to uncertainty in the fault strength parameters, a range of fault strengths representing 'weak', 'average' and 'strong' fault conditions was modelled. Of these models, the average properties are considered to be the most representative for the large faults at Akwaaba. All modelled faults were assumed to be planar and fully persistent, and to have the same strength properties.

Table 4 shows the fault strength parameters. The assumed values for each model were based on the observed infill and large scale characteristics of the faults. For the three models of fault strength, the cohesion and joint stiffness parameters were the same, with the strength difference between the models defined by varying values of friction angle.

The modelling also considered the influence of dilation angle on block stability. For each of the three models of fault strength, a case with dilation (dilation angle = 5°) and a case without dilation (dilation angle = 0°) was modelled.

**Table 1 Assumed material properties for the expected case used to derive rock mass strength**

| Rock Type | UCS (MPa) | E (GPa) | Poisson's Ratio |
|---|---|---|---|
| HW and ore (basalt) | 150 | 96 | 0.32 |
| FW (sandstone) | 243 | 78 | 0.25 |
| FW shear | 126 | 82 | 0.33 |
| Disturbed HW and ore (basalt) | 150 | 96 | 0.32 |
| Disturbed FW (sandstone) | 243 | 78 | 0.25 |
| Disturbed FW shear | 126 | 82 | 0.33 |

**Table 2 Assumed input parameters for the expected case used to derive rock mass strength**

| Rock Type | GSI | $m_i$ | D | $\sigma_{3max}$ (MPa) | Approximate Excavation Depth (m) | Unit Weight ($MN/m^3$) |
|---|---|---|---|---|---|---|
| HW and ore (basalt) | 65 | 11.4 | 0.0 | 7.2 | 500 | 0.029 |
| FW (sandstone) | 65 | 14.2 | 0.0 | 7.0 | 500 | 0.027 |
| FW fault (altered diorite) | 40 | 8.3 | 0.0 | 2.8 | 200 | 0.028 |
| Disturbed HW and ore (basalt) | 65 | 11.4 | 1.0 | 2.0 | 150 | 0.029 |
| Disturbed FW (sandstone) | 65 | 14.2 | 1.0 | 2.0 | 150 | 0.027 |
| Disturbed FW fault (altered diorite) | 40 | 8.3 | 1.0 | 2.0 | 150 | 0.028 |

**Table 3 Expected rock mass strength parameters for each rock type modelled**

| Rock Type | Mohr–Coulomb Failure Envelope | | |
|---|---|---|---|
| | Friction Angle (°) | Cohesion (MPa) | Tensile Strength (MPa) |
| HW and ore (basalt) | 49.0 | 4.24 | 0.936 |
| FW (sandstone) | 54.4 | 5.55 | 1.220 |
| FW shear (altered diorite) | 45.5 | 1.13 | 0.165 |
| Disturbed HW and ore (basalt) | 48.0 | 1.47 | 0.477 |
| Disturbed FW (sandstone) | 53.3 | 1.96 | 0.590 |
| Disturbed FW shear | 30.0 | 0.40 | 0.050 |

**Table 4 Fault strength parameters**

| Fault Strength Model | Joint Normal Stiffness (KN/m) | Joint Shear Stiffness (KN/m) | Cohesion (MPa) | Friction Angle (°) |
|---|---|---|---|---|
| Weak | $1 \times 10^{11}$ | $1 \times 10^{11}$ | 0.01 | 20 |
| Average (expected case) | $1 \times 10^{11}$ | $1 \times 10^{11}$ | 0.01 | 30 |
| Strong | $1 \times 10^{11}$ | $1 \times 10^{11}$ | 0.01 | 40 |

## 4.2 Pre-mining stress state

To date, no stress measurements have been conducted at Akwaaba. The stress field used for all modelling studies conducted at Akwaaba have been extrapolated from the results of a stress measurement programme conducted at Obuasi by Ashanti Goldfields in 1996 (Turner, 1997). The assumed stress field is shown in Table 5.

The magnitude of the major principal stress is approximately 1.7 times the vertical stress and is assumed to be orientated east–west, perpendicular to the major structural features including bedding. The minor principal stress is nearly vertical and equal to the gravitational loading of the overlying strata. The north–south stress is parallel to the shear zone and approximately1.3 times the gravitational load.

**Table 5 Assumed stress state for Akwaaba (based on Turner, 1997)**

| $\sigma_1$ | | | $\sigma_2$ | | | $\sigma_3$ | | |
|---|---|---|---|---|---|---|---|---|
| Gradient (MPa/m) | Trend (°) | Plunge (°) | Gradient (MPa/m) | Trend (°) | Plunge (°) | Gradient (MPa/m) | Trend (°) | Plunge (°) |
| 0.0459 | 95 | 0 | 0.0351 | 5 | 0 | 0.027 | 0 | 90 |

## 4.3 Material models

Both elastic-perfectly plastic and strain-softening material models were used in the FLAC3D and Abaqus models constructed. For the strain softening model, the stress drop following yield was determined from the residual strength properties. The residual strength for each material was assumed to equal 10% of the cohesion, with the friction angle unchanged, equal to the peak properties. Figure 7 shows the strain softening model used in the assessment, which assumes that the residual shear strength is achieved at 0.1% plastic strain ($\varepsilon_p$).

For the 3DEC models, an elastic-perfectly plastic Coulomb slip model was applied to the discontinuities, while the intact rock material was modelled using an elastic isotropic material model, using deformable blocks.

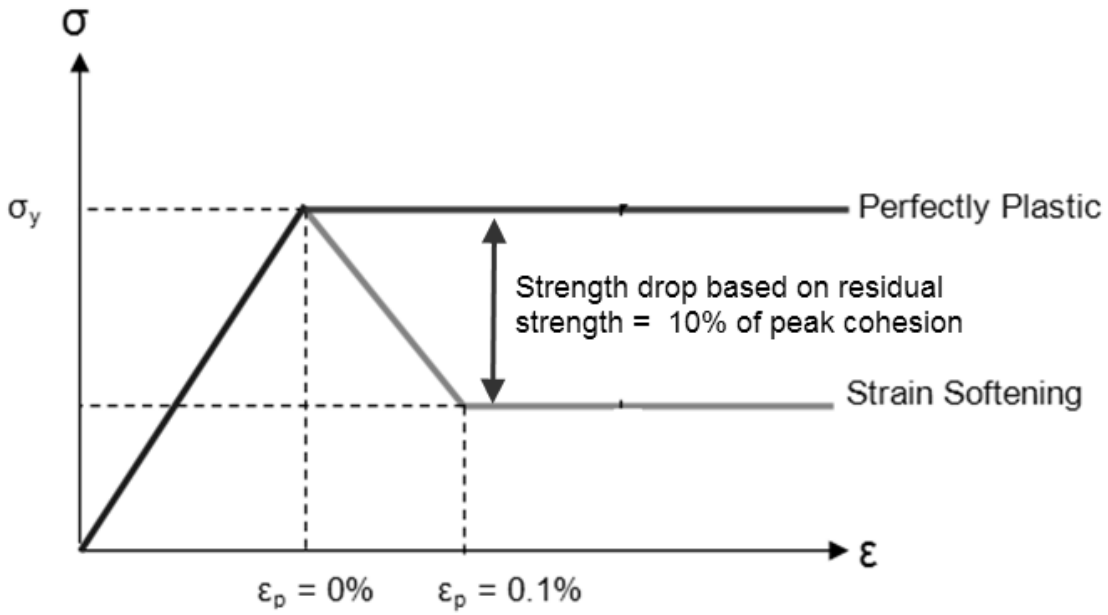


**Figure 7 Strain-softening and perfectly plastic models used in the analysis**

# 5 Numerical modelling results

## 5.1 Crown pillar stability, hangingwall caveability and surface subsidence

The main purpose of the modelling was to assess the stability of the proposed crown pillar, and the likelihood of hangingwall caving for a range of SLC face angles.

Figure 8 shows the zone of modelled yield surrounding the crown pillar using the expected case material properties. The modelling results clearly show that crown pillar failure is unlikely, with only minor amounts of yield observed in the immediate abutments of the SLC and at the base of the pit. This figure also clearly shows that there is no significant zone of yield in the hangingwall of the SLC, indicating that the hangingwall will not cave readily.

Figures 9 and 10 show the extent of yield with the crown pillar removed. It is evident from these figures that even without the crown pillar, the hangingwall of the SLC is unlikely to cave with no significant growth in the zone of yield.

The sensitivity of the hangingwall stability was also assessed, using downgraded properties based on the probable 'worst case' ground conditions. Similar zones of yield were observed using the weaker material model. There was also no noticeable variation in the modelled yield zone between the strain softening and elastic-plastic material models.

The distinct element program 3DEC was also used to assess the potential for hangingwall caving and to identify the location, size and timing of potential unstable rock blocks that could form in the walls of the SLC. The modelling indicated that only a few, relatively small blocks was free to detach from the hangingwall of the SLC for the expected fault properties (Figure 13). This supports the view that the likelihood of the hangingwall continuously caving is low. No significant detached blocks were identified in the footwall of the SLC.

In regard to subsidence, considering the relatively minor amounts of yield observed in the base and sidewalls of the pit (Figures 8 to 10), it unlikely that mining of the SLC will induce any noticeable effects on the surface.

While the modelling indicates that crown pillar failure is unlikely and the hangingwall is not expected to cave, the mine will install comprehensive instrumentation to monitor the hangingwall and crown pillar response.

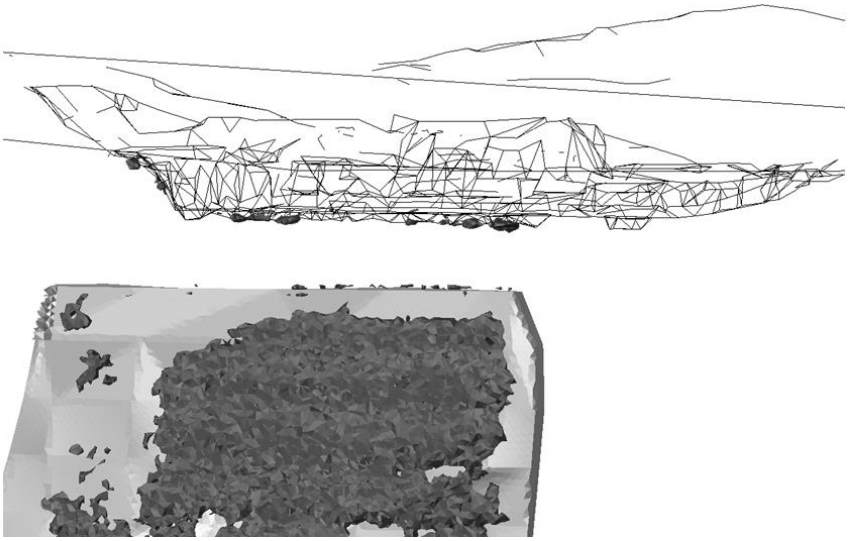

**Figure 8 Long-section showing zone of yield with crown pillar using the expected case material properties. The yield zone is contained within the lower sections of the pit, with no yield observed on the pit surface**

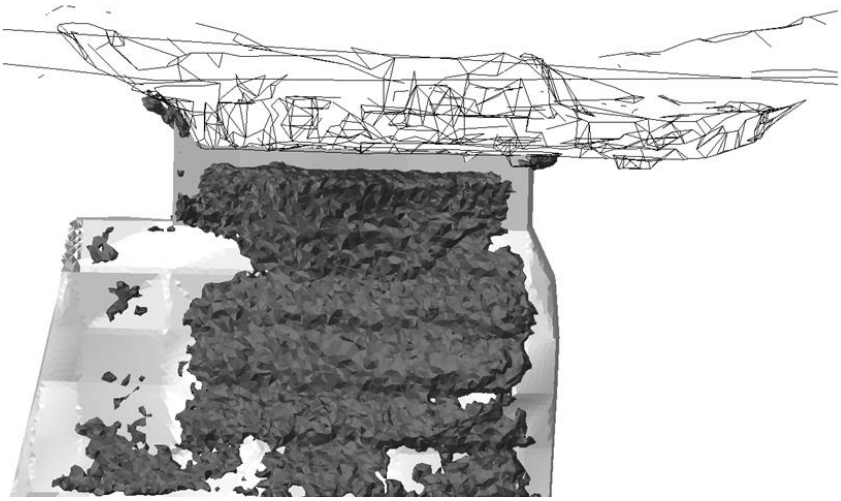

**Figure 9 Long-section showing zone of yield following crown pillar removal using the expected case material properties. The yield zone is contained within the lower sections of the pit, with no yield observed on the pit surface**

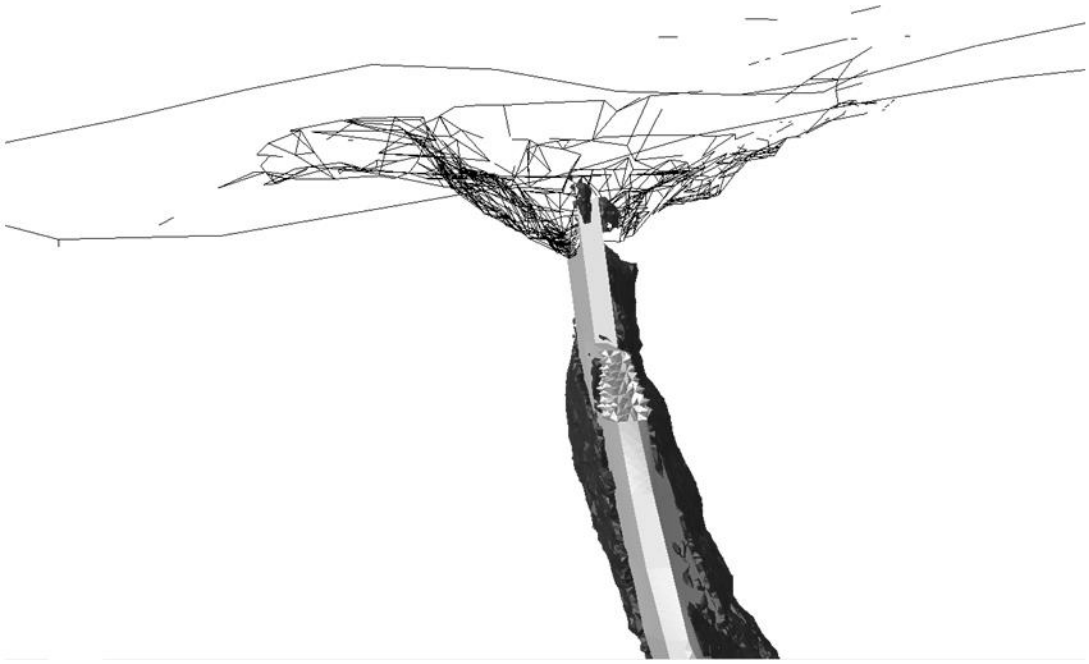

**Figure 10 Cross-section showing zone of yield following crown pillar removal using the expected case material properties**

## 5.3 Extent of yield in the abutments of the SLC

The purpose of this modelling was to assess the extent of rock mass yield in the rock mass surrounding the SLC void for a range of SLC face angles. For this study the SLC extraction sequence was modelled using the finite element code Abaqus. This modelling was conducted in more detail than previous FLAC3D models, incorporating smaller mining steps, a finer element mesh and the use of higher order elements.

The zone of modelled yield for the crown pillar and no-crown pillar options at a typical cross-section is shown in Figure 11 using the expected case material properties. The depth of yield into the HW and FW typically ranges from 5–10 m, although more yield is observed at the top of the SLC near the base of the pit for the case without the crown. There was only a slight increase in the extent of abutment yield, with depths ranging from 10–15 m using the weaker material properties. The modelling indicated no significant variation in the volume of yielded material in the HW and the FW of the SLC for the three face retreat angles considered.

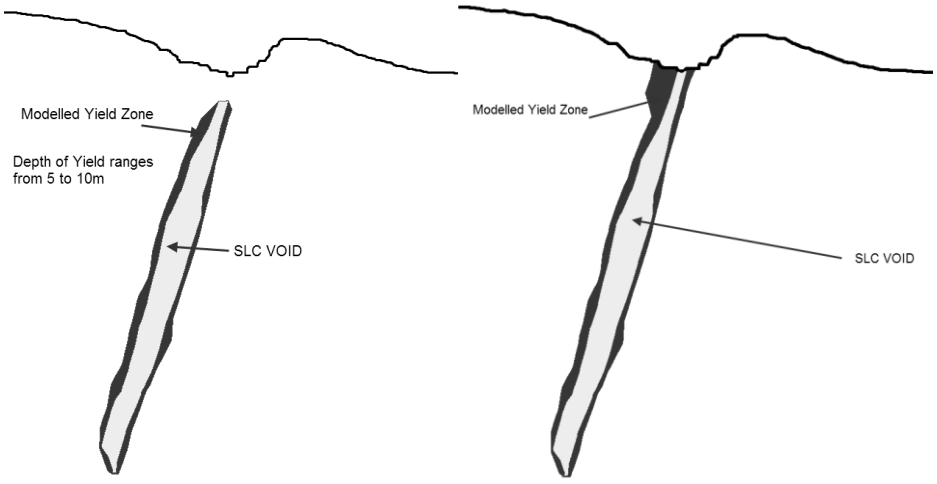


**Figure 11 Cross-sections showing typical depths of yield in the hangingwall and footwall of the SLC void using the expected case material properties**

Figure 12 shows the zone of yield at the modelled brow positions for the three SLC face angles considered. Yield that is occurring in the FW and HW rock mass is not shown in this figure. Similar levels of yield are observed for the top half of the SLC for all face angle options, however, for the bottom half of the SLC there is a noticeable decrease in the extent of yield at the brow for the 60° front.

In the upper levels, the zone of yield typically extends less than 5 m back from the stope brow, while in the lower levels the zone typically extends up to 10 m from the brow.

In the lower levels there is also an increase in the zone of yield below the floor of the SLC void, extending typically 5–10 m below the void. In these locations the toes of the production drill holes are expected to be highly stressed and may be prone to squeezing or shearing.

For brow positions that are highly stressed, cable bolts and additional surface support may be required. If conditions suggest that the rock mass is prone to rockbursting, suitable rockburst-resistant support with dynamic capacity may also be required. This is only expected to be a potential problem for the deeper levels of the mine.

A comparison of the brow conditions for a range of SLC retreat angles indicates that increased yield occurs at the brow for shallower face angles, particularly for the lower levels. A 40–45° face angle is considered to provide the best balance between acceptable brow conditions and reasonable levels of advanced development, whilst maintaining some independence between faces.

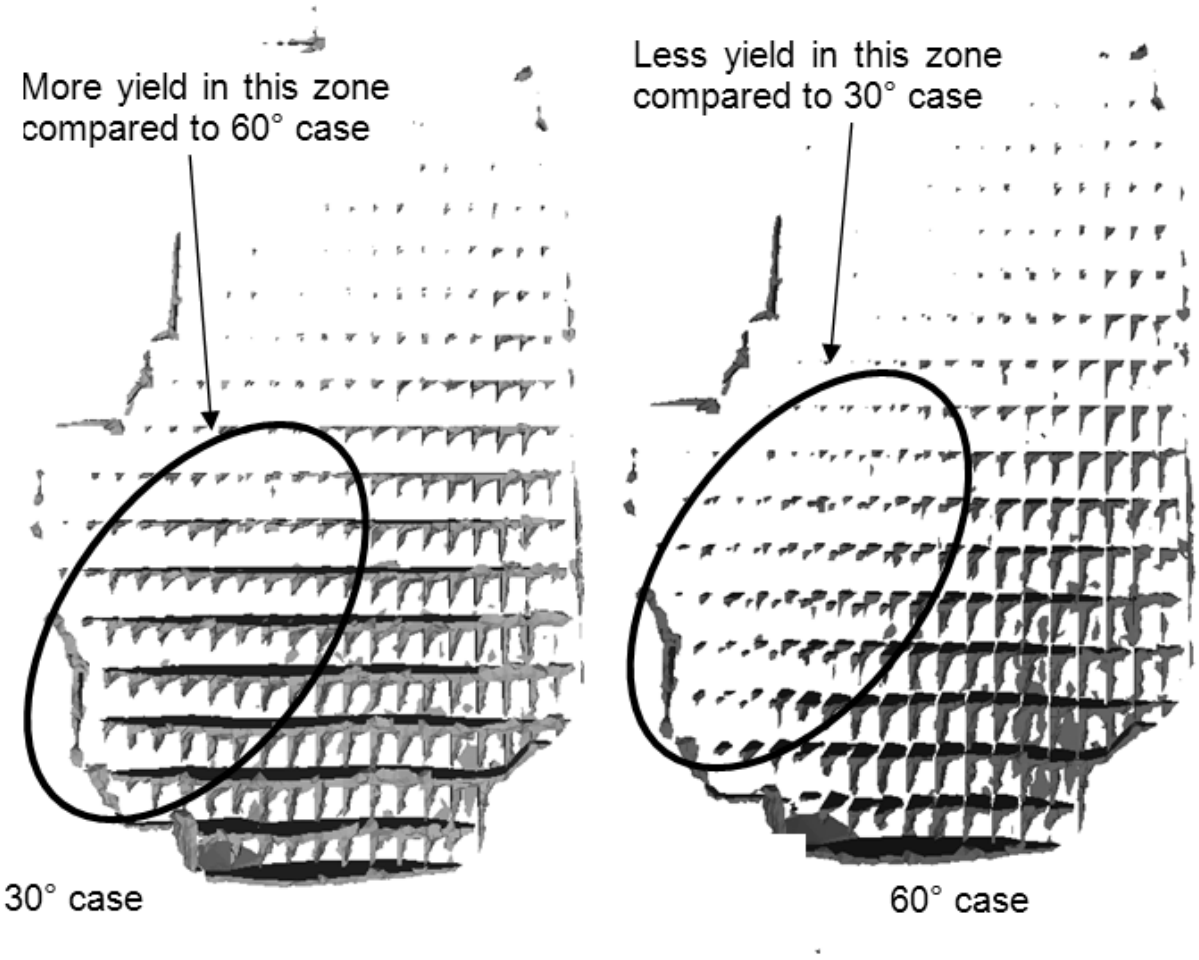


**Figure 12 Zone of modelled yield in the ore zone for 30 and 60° models using the expected case material properties**

## 5.4 Airblast hazard

For this analysis, the numerical modelling programme 3DEC was used. 3DEC is a 3D programme for discontinuum modelling based on the distinct element method. The modelled discontinuities were defined using the large scale continuous fault structures identified from pit and underground mapping, and from interpretation of drill hole logging information.

Figure 13 shows a comparison between the detached blocks (indicated by the dark areas in Figure 13) formed for the 20 and 30° friction angle cases for the two dilation angles considered. There is a significant increase in the number of detached blocks and in the size of the detached zone for the 20° friction angle case without dilation. With dilation, the size of the detached zone for the 20° friction angle case is similar to the other cases. The modelling indicated no noticeable difference in the location, geometry and timing of detached blocks when the friction angle was increased from 30–40°.

While the friction angle = 20° case without dilation indicates a large zone of detached material in the HW, and the possibility of significant HW unravelling, this scenario is considered unlikely. This is further supported by the conservative assumption of fully persistent and planar structures in the model.

For the 30° friction angle case, which better represents the expected fault conditions, the modelling indicated that four small to moderate sized blocks may detach from the HW of the SLC.

Using an analytical expression to calculate the air velocity and air pressure at the draw point locations, the expected sizes of detached blocks from the 3DEC modelling were considered unlikely to induce hazardous airblast conditions. This assumed that a minimum muck pile ‘cushion’ of 75 m is maintained above active draw points. A restricted draw strategy over the first few sublevels and the introduction of low grade ore or waste into the void from the proposed Akwaaba pit will be used to establish and maintain this muck pile cushion.

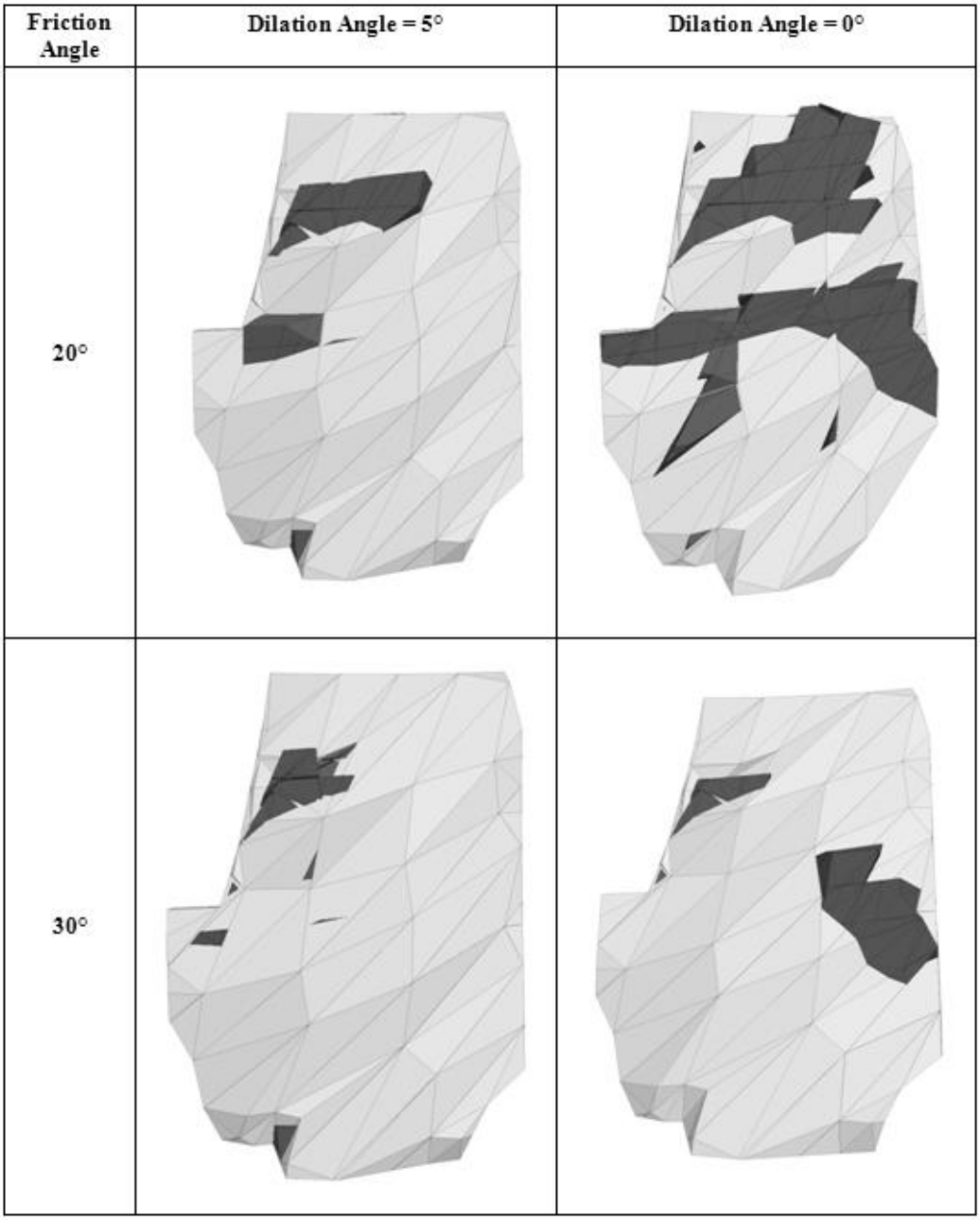


**Figure 13 3DEC model results showing detached blocks for a range of friction and dilation angles**

Also quantified was the expected air velocity and pressures at un-barricaded drives which intersect the SLC void without any muck pile barrier. The timing of block release, the fall height and the geometry of the detached blocks used in the airblast calculations were based on the 3DEC modelling results. Also considered in the assessment was the location of the muck pile at the time of block detachment. The SLC draw sequence was modelled using AMC's stochastic material flow program MFLOW. In most cases at the time of block detachment there was a substantial muck pile height, in excess of the recommended minimum muck pile height of 75 m required to manage the airblast hazard.

This analysis indicated that any block with a cross-sectional area greater than 65% of the SLC void area would result in severe damage, with airblast velocities in excess of 100 m/s expected. These velocities would pose a serious safety hazard and could be expected to cause major damage to equipment and mine infrastructure and fatal injuries to any persons affected.

Although the size of the detached blocks modelled are all considerably less than the 65% of the SLC void area, the decision was made to install airblast barricades in all drives. These barricades have been designed to withstand air pressures up to 1 MPa and will be set back at least 10 m from the brow positions to ensure they are not damaged by the mining induced stress/deformations. The 10 m set back was based on the modelled extent of yield in stope abutments.

The models indicate that the first block forms just prior to the full undercutting of the crown pillar in the model sequence. While the modelling indicates that there is some delay between the start of SLC mining and when the first very large block forms, it was recommended that the barricades are installed as early as possible as precaution and in recognition of the uncertainties in the analysis.

# 6 Conclusions

The results of the modelling study indicated that the proposed crown pillar would be stable for the SLC life of mine extraction sequence.

The modelling also showed that the hangingwall of the SLC is unlikely to cave and that SLC is only expected to induce small scale instabilities in the lower sections of the pit, which are not expected to result in noticeable subsidence on the surface.

The 3DEC modelling results identify a relatively small number of blocks that are prone to detachment from the HW of the SLC. A major airblast hazard is considered highly unlikely at the brows, provided that a minimum muck pile cushion of 75 m is maintained. A restricted draw strategy over the first few sublevels and the introduction of low grade ore or waste into the void from the proposed Akwaaba pit will be used to establish and maintain this muck pile cushion.

While it is unlikely that very large blocks will form, airblast barricades will be installed in all ore drives which intersect the SLC void, at least until there is some confirmation through monitoring that the modelled HW behaviour is representative.

As this is a new mine without any observations and measurement data to calibrate the model material properties, a parametric study using a range of material properties was adopted to reduce the uncertainty in the results. The modelling also considered a number of constitutive models to assess the sensitivity of the model results to a range of post–peak softening responses.

Due to the absence of a stress measurement, there is also some uncertainty in the modelling results. However, considering the relatively low stress environment at the top of the SLC, a change in the stress state is not expected to have a significant impact on the caveability, crown stability or the surface subsidence assessment, which are considered the main geotechnical risks for the project.

To monitor the rock mass response to mining, a comprehensive instrumentation and monitoring system has been designed. This includes the installation of hangingwall and crown pillar monitoring systems, as well as precise levelling across an array of monitoring stations distributed within and outside of the predicted subsidence zone. An over-coring stress measurement will also be conducted at Akwaaba as soon as a suitable underground site is available.

The results of the analyses described above were incorporated into a formal risk assessment to evaluate and rank the inherent risks in the project, including those associated with geotechnical aspects.

# References

Dassault Systèmes (2009) Abaqus/CAE User's Manual, Version. 6.9, Providence, RI, USA: Dassault Systèmes Simulia Corp.

Hoek, E., Carranzato-Torres, C.T. and Corkum, B. (2002) Hoek–Brown failure criterion – 2002 edition, in Proceedings North American Rock Mechanics Society meeting (Toronto, July 2002).

Itasca (2006) User manual for FLAC3D, Version 3.1, Minnesota, Itasca Consulting Group Inc.

Itasca (2007) User manual for 3DEC, Version 4.1, Minnesota, Itasca Consulting Group Inc.

Turner, M.H. (1997) Shaft Rehabilitation and Pillar Extraction at Ashanti Goldfields, SARES97, 1st Southern African Rock Engineering Symposium Proceedings, September 1997.